



Received on 15 October 2024; received in revised form, 08 November 2024; accepted, 14 November 2024; published 01 March 2025

FORMULATION AND EVALUATION OF CLINDAMYCIN PHOSPHATE LOADED CALCIUM CARBONATE NANOPARTICLES FOR TREATING OSTEOMYELITIS

J. Padmapreetha* and U. Mohan Raj

KMCH College of Pharmacy, Coimbatore - 641048, Tamil Nadu, India.

Keywords:

Clindamycin phosphate, Calcium carbonate nanoparticles, Osteomyelitis, Systemic drug delivery, Sustained release

Correspondence to Author:

Dr. J. Padmapreetha

Associate Professor,
KMCH College of Pharmacy,
Coimbatore - 641048, Tamil Nadu,
India.

E-mail: jgmithunseshan@gmail.com

ABSTRACT: This study focuses on developing clindamycin phosphate-loaded calcium carbonate nanoparticles to treat osteomyelitis, utilizing the chemical precipitation method. These nanoparticles were optimized for particle size, zeta potential, drug content, and encapsulation efficiency, resulting in seven different formulations (F1-F7), with formulation F5 was identified as the most effective. Particle size ranged from 275.9 nm to 846.5 nm, and a high homogenization speed of 15,000 rpm was crucial in achieving smaller particle sizes conducive to better bone cell attachment. The zeta potential of -18.8 mV suggested good stability and potential for enhanced interaction with osteoblasts. The optimized formulation F5 exhibited high drug loading (87.56 %) and entrapment efficiency (85.36 %), with FESEM analysis confirming their favorable characteristics for drug delivery. The drug release profile followed a sustained pattern, with 69.60 % of the drug released over 8 hours, adhering to the Higuchi model of quasi-Fickian diffusion. The antimicrobial efficiency tests showed that these nanoparticles could maintain similar inhibitory concentrations against *S. aureus* as the standard clindamycin phosphate solution, indicating effective drug incorporation and sustained release. Overall, clindamycin phosphate-loaded calcium carbonate nanoparticles represent a significant advancement in systemic drug delivery systems for bone infections. The use of biodegradable calcium carbonate not only enhances biocompatibility but also holds promise in reducing healthcare costs and treatment duration. This novel approach of prepared nanoparticles releases the clindamycin phosphate in sustained manner and targeted delivery capabilities to improve treatment outcomes for patients suffering from bone infections.

INTRODUCTION: Prolonged inflammation and infection within the bone are the hallmarks of osteomyelitis, a bone infection that can result from direct trauma, contiguous spread, or hematogenous dissemination^{1, 2, 3}.

Post-traumatic osteomyelitis is a common bone infection disorder that arises from open fractures caused by a traffic accident, a machine injury, or both. It is also the main sign of an open fracture's postoperative infection.

Bacteria that enter the bone tissue after damage and grow rapidly to enormous numbers are easily the cause of osteomyelitis⁴. *S. aureus* is the most frequent pathogenic bacterium among many others that causes chronic osteomyelitis^{7, 8}. Particulate matter with at least one dimension smaller than 100 nm is referred to as a nanoparticle.

QUICK RESPONSE CODE 	DOI: 10.13040/IJPSR.0975-8232.16(3).700-711
	This article can be accessed online on www.ijpsr.com
DOI link: https://doi.org/10.13040/IJPSR.0975-8232.16(3).700-711	

They may consist of organic materials, metal, metal oxides, or carbon¹⁰. Among different inorganic materials, calcium carbonate (CaCO₃) nanoparticles (NPs) have attracted a lot of interest due to their superior biocompatibility and biodegradability, as well as their ease of preparation and pH sensitivity¹¹. The known forms of CaCO₃ are two hydrated metastable phases (calcium carbonate hexahydrate and monohydrocalcite) and three anhydrous crystalline polymorphs (calcite, aragonite, and vaterite)¹². The amorphous calcium carbonate phase is the most soluble of all of them, and it is also the ancestor of anhydrous crystalline polymorphs, which easily crystallize in solutions to form polymorphs¹³. Clindamycin demonstrates excellent bone penetration and oral bioavailability. In a rabbit osteomyelitis model, it has shown comparable efficacy to β -lactam monotherapy. Furthermore, clindamycin has been successfully utilized in the treatment of *Staphylococcus aureus* osteomyelitis in both pediatric and adult populations. The present study aims to formulate and evaluate clindamycin phosphate-loaded calcium carbonate (CP-CaCO₃NPs) nanoparticles as a novel approach for treating osteomyelitis.

MATERIALS AND METHODS: A free gift sample of clindamycin phosphate was obtained from Best Care Pharmaceuticals Pvt. Ltd. Uttarakhand. Calcium carbonate, calcium chloride, sodium carbonate was purchased from Finar chemicals, Hyderabad.

Preparation of Clindamycin Phosphate Loaded Calcium Carbonate Nanoparticles (CP-CaCO₃NPs) by Chemical Precipitation Method: 50 ml of distilled water was used to dissolve calcium chloride, and an aqueous solution of Clindamycin phosphate was magnetically stirred for 15 min at 800 rpm.

After homogenizing the mixture, 50 ml of distilled water were used to dissolve sodium carbonate, which was then added to the mixture drop wise. Until the nanoparticles precipitated, the homogenization process persisted.

5 ml of distilled water were then added to the resulting suspension. To separate the nanoparticles, the suspension was centrifuged for 30 min at 5,000 rpm. A hot air oven was used to dry the nanoparticles^{14,15}.

TABLE 1: COMPOSITION OF CLINDAMYCIN PHOSPHATE LOADED CALCIUM CARBONATE NANOPARTICLES (CP-CaCO₃NPS) BY CHEMICAL PRECIPITATION METHOD

Formulation number	Clindamycin Phosphate (mg)	CaCl ₂ : Na ₂ CO ₃ (g)	Homogenization speed (rpm)	Time of Homogenization (min)
F1	100	2:1	4000	10
F2	100	1:1	8500	20
F3	100	3:1	4000	15
F4	100	2:2	4000	15
F5	100	1:1	15000	25
F6	100	2:1	8500	15
F7	100	1:1	4000	20

Evaluation of Prepared Clindamycin Loaded Calcium Carbonate Nanoparticles:

Preformulation Studies: Preformulation studies were conducted on the clindamycin phosphate, which included solubility, melting point, calibration curve, and FTIR analysis.

Solubility: Clindamycin phosphate solubility was tested using appropriate solvents in accordance with Indian Pharmacopoeia. Clindamycin phosphate's solubility is ascertained by dissolving it in a range of appropriate solvents, including water, ethanol, methanol, and dichloromethane. Clindamycin phosphate is precisely weighed before

being added to the solvent and mixed until it dissolves completely to create the samples¹⁶.

Melting Point: Clindamycin phosphate was filled into one end sealed capillary tube. The filled capillary tube was placed into the melting point apparatus, ensuring it was securely held in place. The sample was gradually heated using the heat source. The rate of heating was slow and steady to allow for accurate observation of the melting point. The temperature displayed on the thermometer was noted when the substance began to melt. It was the melting point of substance¹⁷.

Calibration Curve of Clindamycin Phosphate:

Preparation of Stock Solution: 100 mg of clindamycin phosphate was transferred into a 100 mL volumetric flask to create the standard stock solution. It was dissolved in 100 mL of phosphate buffer (pH 7.4) to produce a stock solution with a 1 mg/mL concentration.

Determination of λ_{\max} of Clindamycin Phosphate:

After identified the analytical wavelength from the standard stock solution, further dilutions were made using phosphate buffer pH 7.4 and the spectrum was overlaid. The phosphate buffer pH 7.4 was used as a blank and the range of 200–400 nm was scanned using a UV-visible spectrophotometer [Shimadzu 1800]. Clindamycin phosphate's lambda max was found to be 210 nm, and this was chosen as the ideal wavelength for detection¹⁸.

Calibration Curve for Clindamycin Phosphate:

The stock solution containing 10 mL of clindamycin phosphate was further diluted to yield a standard solution with a concentration of 100 mg per mL. Utilizing phosphate buffer (pH 7.4), the standard solution was diluted in steps to yield working standard solutions with concentrations of 1, 2, 3, and 5 $\mu\text{g/mL}$. Utilizing a UV visible spectrophotometer and phosphate buffer (pH 7.4) as a blank, the absorbance of the solutions was measured at 210 nm. With concentration ($\mu\text{g/ml}$) on the X-axis and absorbance (nm) on the Y-axis, the calibration curve was plotted.

Compatibility Studies using FT-IR Spectroscopy:

Using the attenuated total reflectance technique, the FT-IR spectra of the pure drug with excipients (1:1 ratio), and CP-CaCO₃NPs were recorded and interpreted for potential chemical interactions between 4000-400 cm^{-1} . For the study, the spectra were scrutinized and evaluated.

Drug Content: A predetermined amount of CP-CaCO₃NPs was dissolved in phosphate buffer (pH 7.4). A 10 $\mu\text{g/mL}$ stock solution was made. Using a UV spectrophotometer (UV-1800, Shimadzu UV Spectrophotometer) set to the wavelength corresponding to the drug's maximum absorbance (210 nm); the absorbance of the resultant solution was measured.

In the same solvent as the CP-CaCO₃NPs, a calibration curve for the drug standard was created. Lastly, calculate the drug content using the formula below.

$$\text{Drug content} = \frac{\text{Analysed clindamycin phosphate concentration}}{\text{Total amount of obtained nanoparticles}} \times 100$$

Drug Entrapment Efficiency: After dissolving 100 mg of the prepared CP-CaCO₃NPs in EDTA and stirring the mixture magnetically for 30 min, 1 mL of water phase was taken, and the absorbance at 210 nm was measured using a UV-visible spectrophotometer to determine the entrapment efficiency. To compute the entrapment efficiency, the provided formula was utilized^{19,20}.

$$\text{EE (\%)} = \frac{\text{wt of initial drug} - \text{wt of free drug}}{\text{wt of initial drug}} \times 100$$

Particle size Analysis: Using Horiba nanoPartica SZ- 100V2 series, the average particle size (z-average) of various CP-CaCO₃NPs formulations was determined. Using dynamic light scattering (DLS), the SZ-100V2 series analyses particle size and particle distribution width. The CP-CaCO₃NPs were scattered in water prior to measurement to obtain the appropriate scattering intensity. Particle size distribution, a crucial parameter for comprehending the physicochemical characteristics and stability of the CP-CaCO₃NPs formulations, was precisely determined thanks to this methodology.

Polydispersity Index: Using the Horiba nanoPartica SZ- 100V2 series, the Polydispersity Index (PDI) of various CP-CaCO₃NP formulations was determined. Using dynamic light scattering (DLS), the SZ-100V2 Series analyses particle size and particle distribution width. The CP-CaCO₃NPs were scattered in water prior to measurement to obtain the appropriate scattering intensity. Particle size distribution is uniform when the PDI is less than 0.5.

Zeta Potential: Using the Horiba nanoPartica SZ- 100V2 series, the zeta potential of various CP-CaCO₃NP formulations was determined. The SZ-100V2 employs a technique called laser Doppler electrophoresis. Surface charge is measured by dynamic light scattering (DLS) in the SZ-100V2 Series.

After being made freshly, the CP-CaCO₃NPs were diluted with distilled water and injected into the zeta-sizer's capillary cell.

FESEM Analysis: FESEM is a crucial instrument for the processes of formulation and development. High-resolution imaging of nanoparticles, displaying their size, shape, and surface morphology, is made possible by FESEM. For FESEM, the optimized formulation (F5) was used. Prior to analysis, gold was sputter-coated onto the prepared CP-CaCO₃NPs dry powder²¹.

In-vitro Drug Release Study: Using USP apparatus II (paddle type) and 900 mL of phosphate buffer pH 7.4 as dissolution medium, *in-vitro* drug release of CP-CaCO₃NPs was carried out at 37 °C with orbital mixing (50 rpm). For eight hours, 3 ml of the medium was removed at predetermined intervals, filtered through a Whatman cellulose acetate membrane with a pore diameter of 20 nm, and replaced with 3 mL of brand-new phosphate buffer (pH 7.4). Using a UV-visible spectrophotometer set at 210 nm, the amount of liberated clindamycin phosphate from calcium carbonate nanoparticles was quantified. Cumulative percent drug release was computed using the data that was obtained²¹.

Kinetic Modeling of the Drug Release: The resultant release data were fitted into four mathematical models including zero-order model, first-order model, Higuchi model, Korsmeyer – Peppas to determine the mechanism of drug release²².

Determination of Minimum Inhibitory Concentrations for Anti-microbial Activity (MICs): MICs were calculated using the MIC method of serial dilution. The accepted technique for figuring out an antibiotic's level of resistance is the tube dilution test. An antibiotic is serially diluted in a liquid medium that has been inoculated with a fixed number of organisms and left to incubate for a predetermined amount of time. The minimal inhibitory concentration (MIC) of an antibiotic is the lowest concentration (highest dilution) that prevents the appearance of turbidity. The antibiotic is bacteriostatic at this dilution.

RESULTS:

Solubility: Solubility tests were carried out with a variety of solvents, including ethanol, water, and dichloromethane. To evaluate Clindamycin Phosphate's solubility, visual inspections were conducted.

TABLE 2: SOLUBILITY STUDY OF CLINDAMYCIN PHOSPHATE

Solvent	Parts of solvent required to dissolve one part of solute	Observation	Result
Water	1 to 10 parts	Freely soluble	Complies with Indian pharmacopoeia 2022 Volume I
Ethanol	1000 to 10000 parts	Very slightly soluble	
Dichloromethane	More than 10000 parts	Practically insoluble	

Melting Point: The capillary method and the instrument melting point apparatus were used to determine the melting point of pure drug.

Clindamycin phosphate's melting point, which was determined to be 142°C, is within the 141–143 °C range that Merck's index mentions.



FIG. 1: MELTING POINT OF CLINDAMYCIN PHOSPHATE

Calibration Curve of Clindamycin Phosphate:

Determination of Absorption Maximum: With a blank, the sample containing 10 µg/mL of clindamycin phosphate was scanned in the 200–400 nm range using a UV–VIS Spectrophotometer. The wavelength that corresponded to the maximum absorbance (λ_{max}) was then recorded. The sample's absorbance peaked at 210 nm in wavelength.

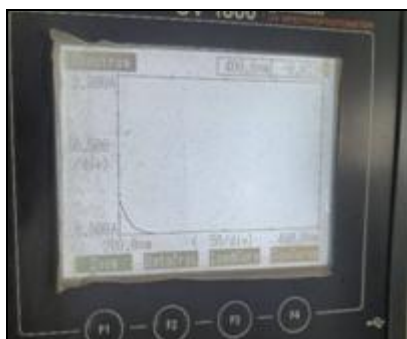


FIG. 2: ABSORPTION MAXIMA SPECTRA OF CLINDAMYCIN PHOSPHATE

Construction of Calibration Curve:

TABLE 3: ABSORBANCE OF CLINDAMYCIN PHOSPHATE AT 210 NM

Concentration (µg/ml)	Absorbance at 210 nm
0	0
1	0.071
2	0.12
3	0.18
4	0.234
5	0.3

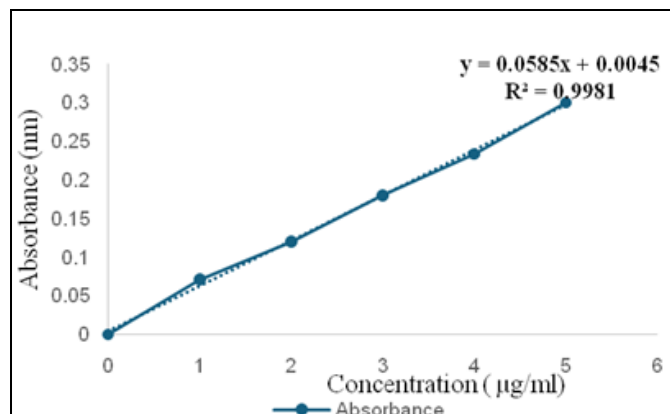


FIG. 3: CALIBRATION CURVE OF CLINDAMYCIN PHOSPHATE

With an R^2 value of 0.9981, the standard concentration of clindamycin phosphate at 210 nm demonstrated good linearity, indicating that Beer-Lambert's law is followed.

Drug Excipient Compatibility Studies using FT-IR Spectroscopy:

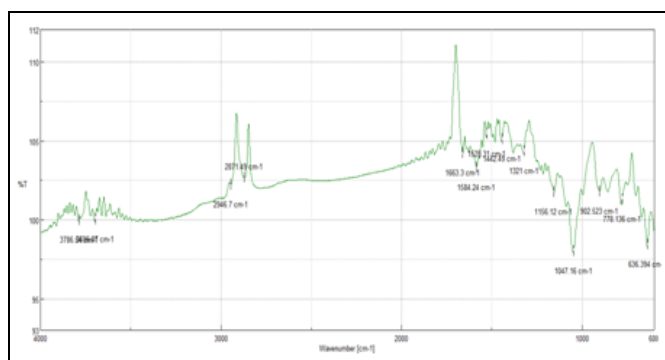


FIG. 4: FT-IR SPECTRUM OF CLINDAMYCIN PHOSPHATE

TABLE 4: FT-IR CHARACTERISTIC SPECTRAL DETAILS OF CLINDAMYCIN PHOSPHATE

Wave Number (cm ⁻¹)	Functional Group
1047	C-O stretching vibration
1321	P=O stretching vibration
1442	C-H bending vibration
1446	O-H bending vibration
1663	C=O stretching vibration
3786,3460,3696	O-H stretching vibrations

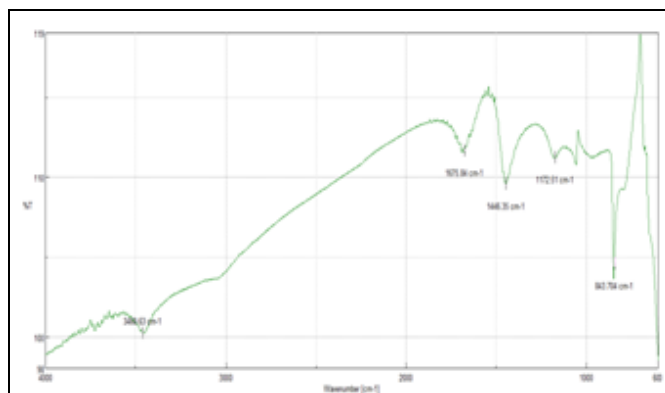


FIG. 5: FT-IR SPECTRUM OF CALCIUM CHLORIDE

TABLE 5: FT-IR CHARACTERISTIC SPECTRAL DETAILS OF CALCIUM CHLORIDE

Wave Number (cm ⁻¹)	Functional Group
843	Ca-Cl stretching vibration
1172	C-N stretching vibration
1446	O-H bending vibration
1675	C=O stretching vibration
3460	O-H stretching vibrations

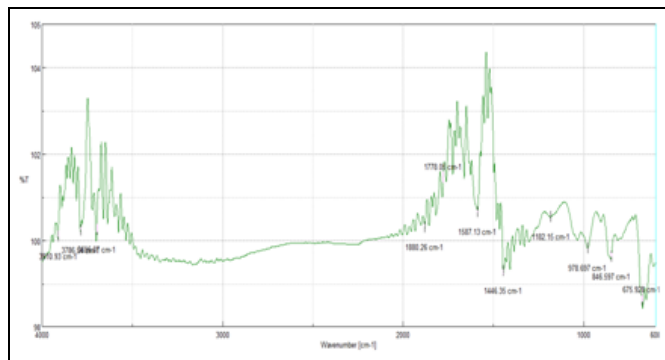
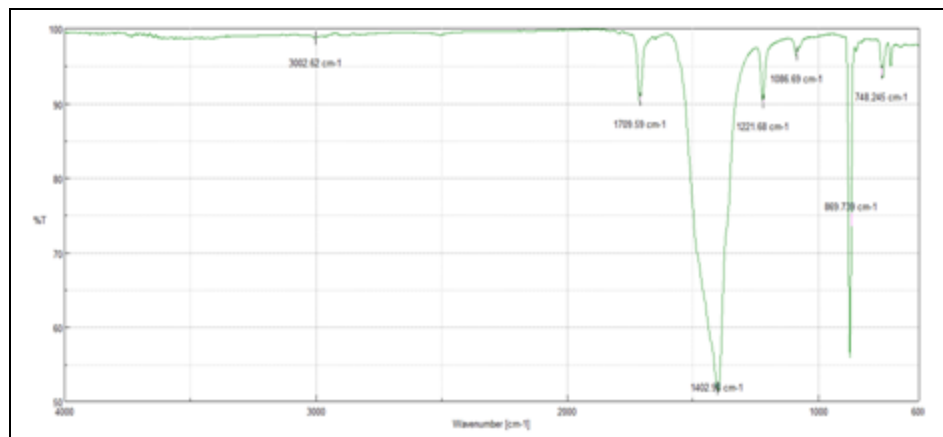


FIG. 6: FT-IR SPECTRUM OF SODIUM CARBONATE

TABLE 6: FT-IR CHARACTERISTIC SPECTRAL DETAILS OF SODIUM CARBONATE

Wave Number (cm ⁻¹)	Functional Group
978	C-O bending vibration
1182	C-O stretching vibration
1446	O-H bending vibration
1778	C=O stretching vibration
3002	O-H stretching vibrations

**FIG. 7: FT-IR SPECTRUM OF CLINDAMYCIN PHOSPHATE LOADED CALCIUM CARBONATE NANOPARTICLES****TABLE 7: FT-IR PEAKS OF DRUG, EXCIPIENTS, AND FORMULATIONS**

Functional groups	Wave Number (cm ⁻¹)			
	DRUG	CaCl ₂	Na ₂ CO ₃	NPs
C-O stretching vibration	1047	1221	1182	1321
P=O stretching vibration				1321
C-H bending vibration	1442	869	1442	
N-H bending vibration				1584
C=O stretching vibration	1663		1675	1709
O-H stretching vibrations	3786,3460,3696		3002	
Ca-Cl stretching vibration		843		
C-N stretching vibration				1172
O-H bending vibration	1446		1446	1402
C-O bending vibration	978			

The drug and the nanoparticles infrared spectra were compared. The functional peaks in the drug, calcium chloride, and sodium carbonate spectra did not significantly differ from one another, according to the study. The lack of new peaks produced by nanoparticles suggests that the drug and excipient are compatible. We concluded that the drug and its excipients get interacted with each other.

Drug Content: All prepared CP-CaCO₃NPs formulations (F1 through F7) had varying drug contents, ranging from 79.35 % to 84.64 %. Comparing formulation F5 to formulations with lower concentrations, the former showed a noticeably higher drug content. The values are typically regarded as appropriate for a hydrophilic medication like CP. The range of the prepared CP-CaCO₃ NPs formulations was 72.5-87.56 %.

Moreover, a crucial factor governing the effectiveness of drug loading is the particle surface charge.

TABLE 8: PERCENTAGE DRUG CONTENT OF F1-F7 FORMULATIONS

Formulation	Drug content (%)
F1	79.35
F2	84.64
F3	72.5
F4	75.23
F5	87.56
F6	75.98
F7	76.2

Entrapment Efficiency: The entrapment efficiency of all prepared CP-CaCO₃NPs formulations (F1 to F7) varied between 68.32 % , 77.28 % , 70.10 % , 72.10 % , 85.36 % , 69.98 % , 71.04 % as shown in the **Table 9**. Formulation F5

exhibited significantly higher entrapment efficiency compared to other formulations with lower entrapment efficiency. The entrapment efficiency of prepared nanoparticles were in the range of 68.32 to 85.36 %.

TABLE 9: PERCENTAGE ENTRAPMENT EFFICIENCY OF F1-F7 FORMULATIONS

Formulation	Drug entrapment efficiency (%)
F1	68.32
F2	77.28
F3	70.10
F4	72.10
F5	85.36
F6	69.98
F7	71.04

Due to the drug's quick diffusion into the aqueous phase, conventional techniques for creating hydrophilic drug nanoparticles have low drug entrapment during the preparation phase. This study employed a chemical precipitation method to increase loading efficiency. High encapsulation efficiencies for hydrophilic medications are offered by this technique.

Particle size Analysis: From the results obtained, all the CP-CaCO₃NPs formulations were within the nanometer size range. The particle size of all the formulated nanoparticles was found to be in the range of 275.9 nm – 846.5 nm. Formulation F5 significantly exhibited particle size (275.9 nm) compared to other formulations with higher particle size. The effect of Homogenization revealed that the high homogenization speed (15,000 rpm) increased both mechanical and hydraulic shear, which in turn could effectively reduce the particle size.

TABLE 10: PARTICLE SIZE OF F1-F7 FORMULATIONS

Formulation	Particle size (nm)
F1	673
F2	411.5
F3	846.5
F4	625.3
F5	275.9
F6	691
F7	432

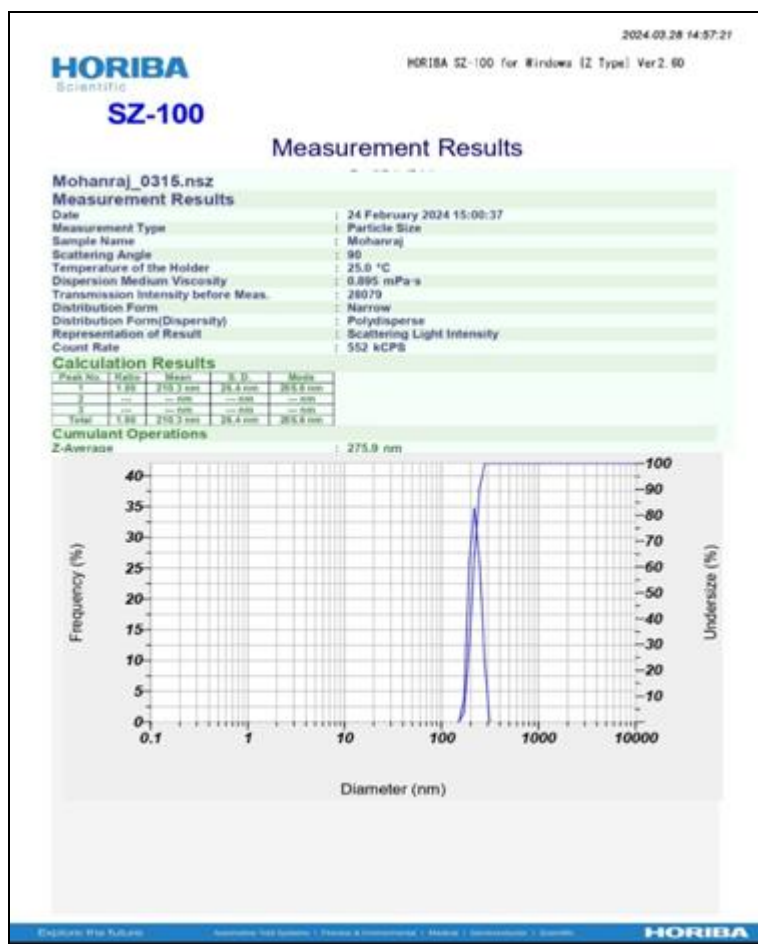


FIG. 8: PARTICLE SIZE OF FORMULATION F5

Polydispersity Index: PDI reflected the uniformity of particle size distribution within a sample. Lower PDI values indicated a more uniform distribution, which was desirable for consistent drug delivery. The polydispersity index of all CP-CaCO₃NPs formulations was found to be in the range of 0.356 – 0.498. Formulation F5 significantly exhibited polydispersity index (0.356) compared to other formulations with higher polydispersity index. PDI below 0.5 indicates uniform particle size distribution.

Zeta Potential: Zeta potential reflected the surface charge of nanoparticles and played a role in their stability and interactions with biological membranes. Zeta potential can also be used to determine whether an active material (such as drug) is incorporated within or absorbed on the surface of the nanoparticle.

Zeta potential range of approximately ± 30 mV or higher was often considered desirable for ensuring colloidal stability and preventing particle aggregation. The average zeta potential of Clindamycin phosphate -loaded Calcium carbonate nanoparticles of Formulation F2 and F5 was found to be -21.0 mV & -18.8 mV. It has been proposed that negative values of the zeta potential have an important favorable effect on the attachment and proliferation of the bone cells. Formulation F5 shows the favorable zeta potential of -18.8 mV compared to other formulations.

TABLE 11: POLYDISPERSITY INDEX OF F1-F7 FORMULATIONS

Formulation	Polydispersity index
F1	0.412
F2	0.379
F3	0.475
F4	0.409
F5	0.356
F6	0.463
F7	0.401

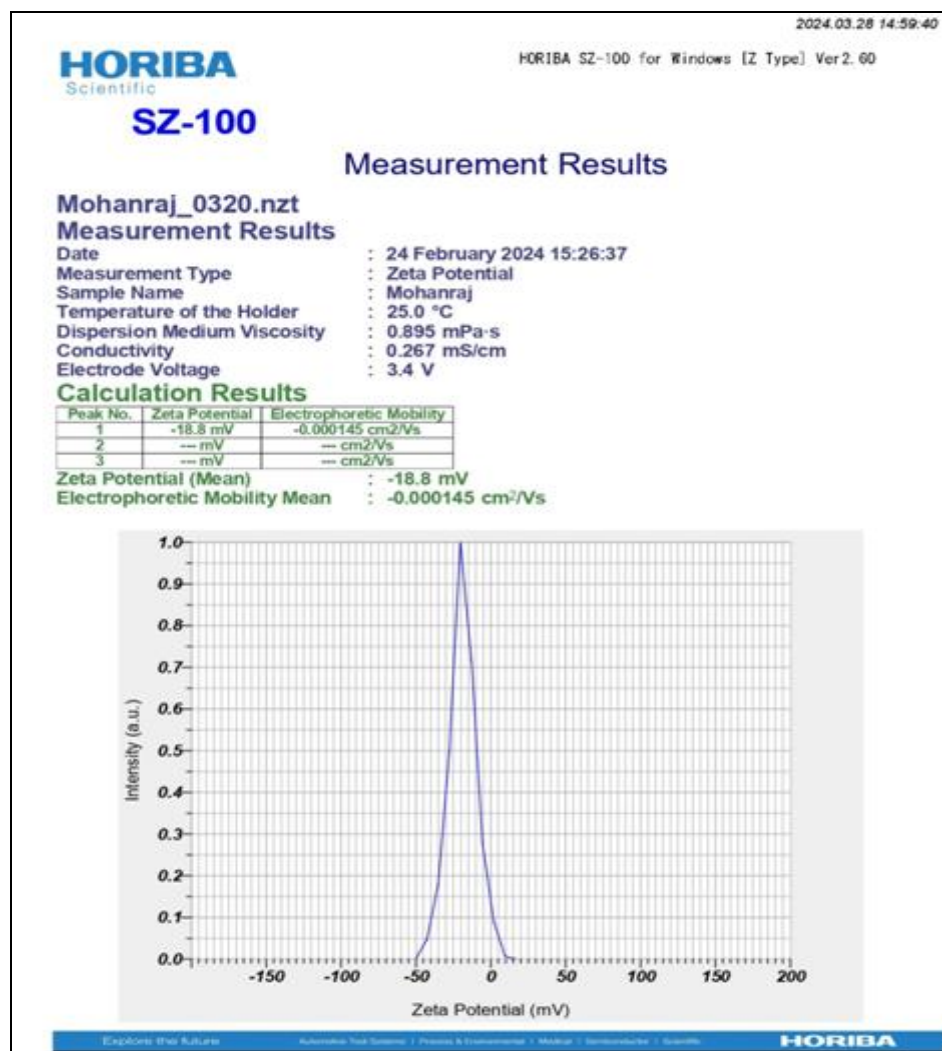


FIG. 9: ZETA POTENTIAL OF FORMULATION F5

Optimized Formulation: After careful evaluation of drug content, and entrapment efficiency, particle size, zeta potential, Formulation F5 emerged as the optimized choice. F5 displayed the most desirable characteristics among all tested formulations. Its particle size (275.9 nm) was within the desired range for oral drug delivery. Additionally, F5 exhibited a favorable zeta potential (-18.8), ensuring stability and dispersion uniformity. Furthermore, its high drug content (87.56 %) and entrapment efficiency (85.36 %) indicated efficient encapsulation of the therapeutic agent, making F5 the ideal candidate for further evaluation.

FESEM Analysis: Particle size and morphology of CP-CaCO₃NPs were studied by scanning electron microscopy (SEM). The SEM image of the optimized Formulation F5 was shown in Figure exhibit the typical morphological aspects of nanoparticles. Particles were found to be crystal structure and CP-CaCO₃NPs were mainly well-dispersed, uniformly sized & cluster of regularly shaped crystals.

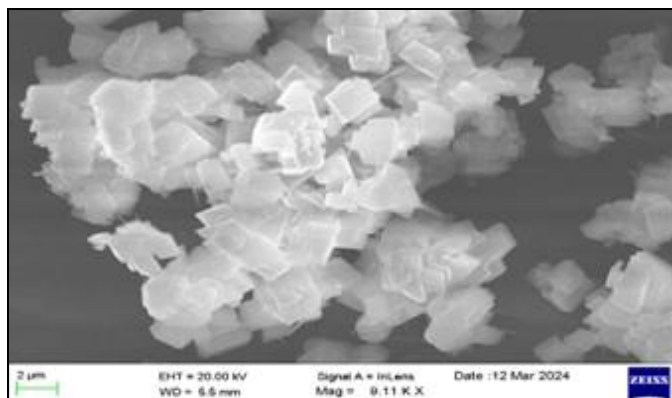


FIG. 10: SCANNING ELECTRON MICROSCOPY IMAGE OF F5 - CP-CaCO₃NPS

In-vitro Drug Release Study: USP apparatus II, a paddle-type device, was used to conduct a drug release study of the optimized formulation F5. Following an 8 h study, the percentage of clindamycin phosphate released from calcium carbonate nanoparticles was found to be 69.50 % for formulation F5, the optimized formulation. The prolonged release of clindamycin phosphate from CP-CaCO₃NP suggests that improved

microenvironment created by entrapment efficiency of clindamycin phosphate into nanoparticles causes a slower release of clindamycin phosphate over an extended period of time.

TABLE 12: PERCENTAGE CUMULATIVE DRUG RELEASE OF CP-CaCO₃NPS

Time (min)	Percent cumulative drug release
30	9.39
60	18.15
90	24.44
120	29.77
150	34.52
180	37.50
210	40.26
240	43.68
270	47.40
300	52.12
360	57.56
420	63.39
480	69.60

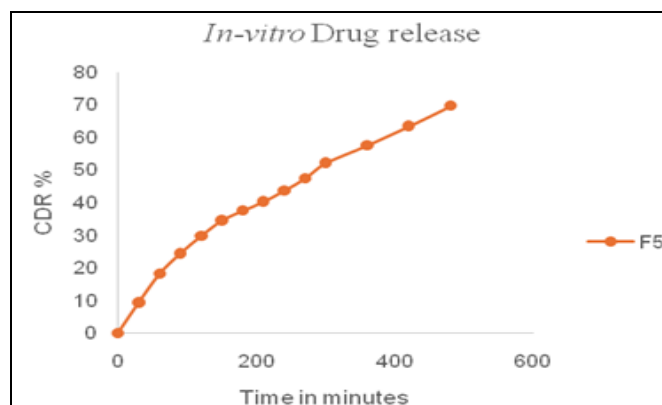


FIG. 11: IN-VITRO DRUG RELEASE STUDY OF CP-CaCO₃NPS

Kinetic Modeling of the Drug Release: In order to investigate the drug release pattern and mechanism, the optimized formulation F5 of clindamycin Phosphate-loaded calcium carbonate nanoparticles (CP-CaCO₃NPs), was performed.

The percentage drug release data was analyzed with the mathematical models Zero order, first order, Higuchi and korsmeyer peppas plot. The preference of a certain mechanism was based on the coefficient of determination (r^2) for the parameters studied, where the highest coefficient of determination is preferred for the selection of the order of release.

TABLE 13: MATHEMATICAL MODELS OF IN-VITRO RELEASE DATA OF CLINDAMYCIN PHOSPHATE-LOADED CALCIUM CARBONATE (CP-CaCO₃NPS) NANOPARTICLES

Sample	Zero order R^2	First order R^2	Higuchi model R^2	Korsmeyer-Peppas model	
				R^2	n' value
F5	0.9751	0.9501	0.9927	0.8699	0.2121

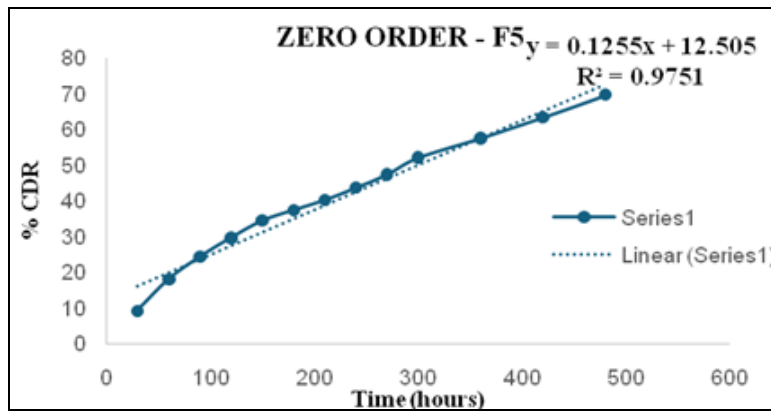


FIG. 12: MATHEMATICAL MODELS OF *IN-VITRO* RELEASE DATA CLINDAMYCIN PHOSPHATE-LOADED CALCIUM CARBONATE (CP-CACO₃NPS) NANOPARTICLES (ZERO ORDER)

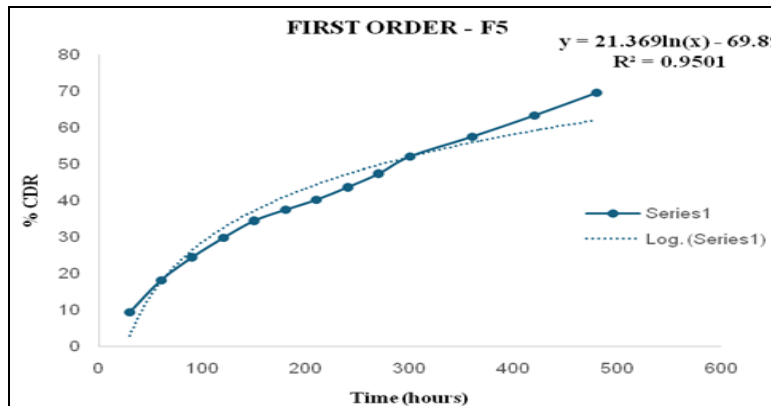


FIG. 13: MATHEMATICAL MODELS OF *IN-VITRO* RELEASE DATA CLINDAMYCIN PHOSPHATE-LOADED CALCIUM CARBONATE (CP-CACO₃NPS) NANOPARTICLES (FIRST ORDER)

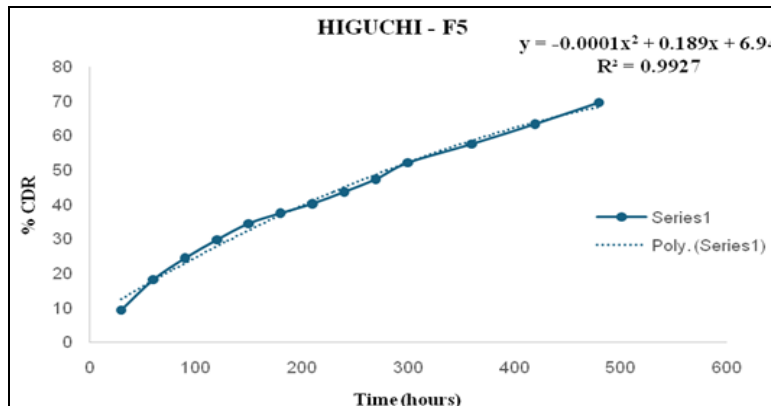


FIG. 14: MATHEMATICAL MODELS OF *IN-VITRO* RELEASE DATA CLINDAMYCIN PHOSPHATE-LOADED CALCIUM CARBONATE (CP-CACO₃NPS) NANOPARTICLES (HIGUCHI)

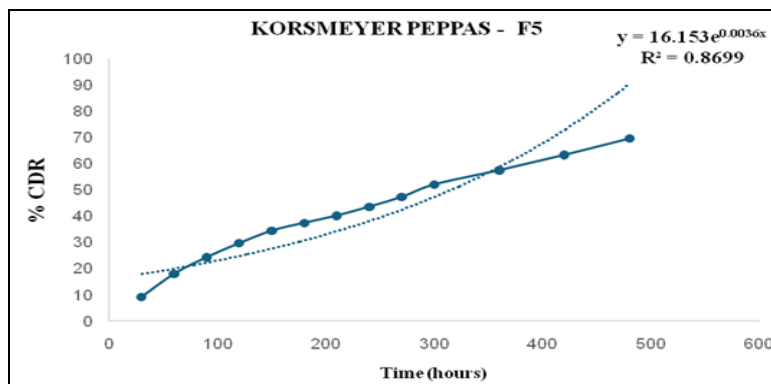


FIG. 15: MATHEMATICAL MODELS OF *IN-VITRO* RELEASE DATA CLINDAMYCIN PHOSPHATE-LOADED CALCIUM CARBONATE (CP-CACO₃NPS) NANOPARTICLES (KORSMEYER PEPPAS)

Specifically, for the optimized formulation (F5), the Higuchi model demonstrated the highest correlation coefficient ($R^2=0.9927$), indicating its superior fit. The Higuchi model explains the release of drugs from insoluble matrix as a square root of time-dependent process based on Fickian diffusion equation. Additionally, the determination of the release exponent "n" value as 0.2121 through the Korsmeyer-Peppas model further supported the conclusion of a diffusion-controlled release mechanism, commonly known as quasi-Fickian diffusion. The determined n-value, being less than 0.5, indicated a drug release mechanism leaning towards quasi-Fickian diffusion.

Antimicrobial Efficiency: For the tested *S. aureus* species, the MIC value of the CP solution was found to be 6 $\mu\text{g/mL}$; based on the CLSI protocol, this strain could be classified as sensitive. To determine if the optimized formulation (F5) of the prepared CP- CaCO_3 NPs was active against *S. aureus*, tests were conducted. After two days of culture incubation, a reduction in the growth extent of *S. aureus* was observed for the CaCO_3 nanoparticles loaded with CP. Presumably, the long-term released characteristics of CP- CaCO_3 NPs adsorbed to the microorganisms cell surface can function as a drug depot to slow down the bacteria's rate of growth. The promising properties of CaCO_3 nanoparticles as a drug carrier can therefore be used to deliver clindamycin phosphate with advantage.

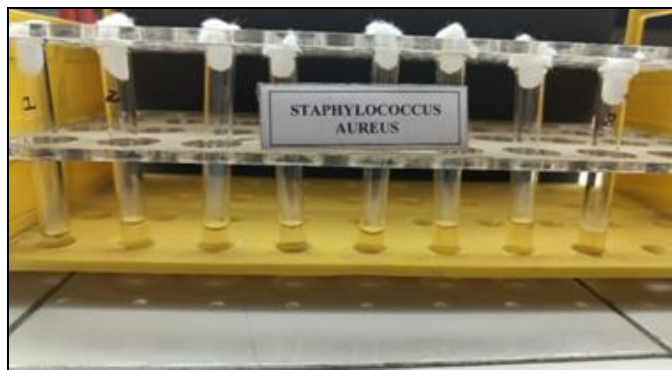


FIG. 16: ANTIMICROBIAL EFFICIENCY OF CLINDAMYCIN PHOSPHATE-LOADED CALCIUM CARBONATE (CP- CaCO_3 NPS) NANOPARTICLES-OPTIMIZED FORMULATION (F5) AGAINST *S. AUREUS*

Thus, our prepared nano-formulations with antimicrobial efficiency can be a potential systemic drug delivery system for bone infection disease.

Designing sustained release CP loaded nanoparticles using a biodegradable and osteoconductive material such as CaCO_3 a promising expectation for bone infection therapy.

CONCLUSION: In conclusion, the development of clindamycin phosphate-loaded calcium carbonate nanoparticles shows promise for treating osteomyelitis and other bone infections. Optimizing particle size, zeta potential, drug content, and encapsulation efficiency enhances their effectiveness as drug carriers. The use of biodegradable materials like calcium carbonate improves biocompatibility and may reduce treatment costs and duration. *In-vitro* studies demonstrated sustained drug release over an extended period. This technology represents a significant advancement in drug delivery, offering potential benefits for improving treatment outcomes and patient care in managing bone infections. In summary, clindamycin phosphate-loaded calcium carbonate nanoparticles offer a novel and effective approach for treating bone infections with more bioavailability.

ACKNOWLEDGEMENT: Nil

CONFLICTS OF INTEREST: Nil

REFERENCES:

1. Masters EA, Ricciardi BF, De Mesy Bentley KL, Moriarty TF, Schwarz EM and Muthukrishnan G.: Skeletal infections: microbial pathogenesis, immunity and clinical management. *Nature Reviews Microbiology* 2022; 385–400.
2. Urish KL and Cassat JE: Staphylococcus aureus osteomyelitis: bone, bugs, and surgery. *Infection and Immunity* 2020; 88(7): 10-128.
3. Panteli M and Giannoudis PV: Chronic osteomyelitis: what the surgeon needs to know. *EFORT Open Reviews* 2016; 128–135.
4. Kavanagh N, Ryan EJ, Widaa A, Sexton G, Fennell J, O'Rourke S, Cahill KC, Kearney CJ, O'Brien FJ and Kerrigan SW: Staphylococcal osteomyelitis: disease progression, treatment challenges, and future directions. *Clin Microbiol Rev* 2018; 31(2): 00084-17.
5. Lima AL, Oliveira PR, Carvalho VC, Cimerman S and Savio E: Diretrizes Panamericanas para el Tratamiento de las Osteomielitis e Infecciones de Tejidos Blandos Group. Recommendations for the treatment of osteomyelitis. *Braz J Infect Dis* 2014; 18(5): 526-34.
6. McNeil JC, Vallejo JG, Kok EY, Sommer LM, Hultén KG and Kaplan SL: Clinical and microbiologic variables predictive of orthopedic complications following *Staphylococcus aureus* acute hematogenous osteoarticular infections in children. *Clin Infect Dis* 2019; 69(11): 1955-1961.

7. Saadatian-Elahi M, Teysou R and Vanhems P: *Staphylococcus aureus*, the major pathogen in orthopaedic and cardiac surgical site infections: a literature review. Int J Surg 2008; 6(3): 238-45.
8. Wang X, Yu S, Sun D, Fu J, Wang S, Huang K and Xie Z: Current data on extremities chronic osteomyelitis in southwest China: epidemiology, microbiology and therapeutic consequences. Sci Rep 2017; 7(1): 16251.
9. Savita Kumari and Leena Sarkar: A Review on Nanoparticles: Structure, Classification, Synthesis & Applications. J of Scientific Research 2021; 8(65): 42-46.
10. Qi C, Lin J, Fu LH and Huang P: Calcium-based biomaterials for diagnosis, treatment, and theranostics. Chem Soc Rev 2018; 47(2): 357-403.
11. Cartwright JH, Checa AG, Gale JD, Gebauer D and Sainz-Díaz CI: Calcium carbonate polyamorphism and its role in biomineralization: how many amorphous calcium carbonates are there? Angew Chem Int Ed Engl 2012; 51(48): 11960-70.
12. Wolf SE, Leiterer J, Kappl M, Emmerling F and Tremel W: Early homogenous amorphous precursor stages of calcium carbonate and subsequent crystal growth in levitated droplets. JACS 2008; 130(37): 12342-7.
13. Dizaj SM, Lotfipour F, Barzegar-Jalali M, Zarrintan MH, Adibkia K. Box-Behnken experimental design for preparation and optimization of ciprofloxacin hydrochloride-loaded CaCO₃ nanoparticles. Journal of Drug Delivery Science and Technology 2015; 29: 125-31.
14. Indian pharmacopoeia. Clindamycin Phosphate published by The Indian pharmacopoeia commission Ghaziabad, edition 9, effective from 1st 2022; 1: 272.
15. The Merck Index: An Encyclopedia of Chemicals, Drug, and Biologicals, 15th Edition Edited by Maryadele J. O'Neil, Royal Society of chemistry, Cambridge, UK ISBN 9781839736701.
16. Nataraj KS, Raju GN and Narasimha Surya AB: UV spectrophotometric method development for estimation of clindamycin phosphate in bulk and dosage form. Int J Pharm Biol Sci 2013; 3: 164-167.
17. Qian K, Shi T, Tang T, Zhang S, Liu X and, Cao Y: Preparation and characterization of nano-sized calcium carbonate as controlled release pesticide carrier for validamycin against *Rhizoctonia solani*. Microchimica Acta 2011; 173: 51-7.
18. Ueno Y, Futagawa H, Takagi Y, Ueno A and Mizushima Y: Drug-incorporating calcium carbonate nanoparticles for a new delivery system. J of Contr Rele 2005; 103(1): 93-98.
19. Maleki Dizaj S, Lotfipour F, Barzegar-Jalali M, Zarrintan MH and Adibkia K: Ciprofloxacin HCl-loaded calcium carbonate nanoparticles: preparation, solid state characterization, and evaluation of antimicrobial effect against *Staphylococcus aureus*. Artif Cells Nanomed Biotechnol 2017; 45(3): 535-543.
20. Barzegar-Jalali M, Valizadeh H, Nazemiyeh H, Barzegar-Jalali A, Shadbad MRS, Adibkia K and Zare M: Reciprocal powered time model for release kinetic analysis of ibuprofen solid dispersions in oleaster powder, microcrystalline cellulose and crospovidone. J Pharma Pharm Sci 2010; 13: 152-161.

How to cite this article:

Padmapreetha J and Raj UM: Formulation and evaluation of clindamycin phosphate loaded calcium carbonate nanoparticles for treating osteomyelitis. Int J Pharm Sci & Res 2025; 16(3): 700-711. doi: 10.13040/IJPSR.0975-8232.16(3).700-711.

All © 2025 are reserved by International Journal of Pharmaceutical Sciences and Research. This Journal licensed under a Creative Commons Attribution-NonCommercial-ShareAlike 3.0 Unported License.

This article can be downloaded to **Android OS** based mobile. Scan QR Code using Code/Bar Scanner from your mobile. (Scanners are available on Google Playstore)